Available online at www.sciencedirect.com
ScienceDirect
Journal of Power Sources 159 (2006) 38–41
JOURNAL OF POWER SOURCES
www.elsevier.com/locate/jpowsour

Short communication

Microwave-induced combustion synthesis and electrical properties of $Ce_{1-x}Sm_xO_{2-1/2x}$ ceramics

Yen-Pei Fu [a,*], Cheng-Hsiung Lin [b], Chung-Wen Liu [b], Kok-Wan Tay [c], Shaw-Bing Wen [d]

[a] Department of Materials Science and Engineering, National Dong-Hwa University, Shou-Feng, Hualien 974, Taiwan
[b] Department of Chemical Engineering, Wu-Feng Institute of Technology, Ming-Hsiung, Chiayi 621, Taiwan
[c] Department of Electrical Engineering, Wu-Feng Institute of Technology, Ming-Hsiung, Chiayi 621, Taiwan
[d] Department of Resources Engineering, National Cheng Kung University, Tainan 701, Taiwan

Available online 5 June 2006

Abstract

$Ce_{1-x}Sm_xO_{2-1/2x}$ nanopowders were successfully synthesized by microwave-induced combustion process. For the preparation, cerium(III) nitrate hexahydrate, samarium(III) nitrate hexahydrate, and urea were used for the microwave-induced combustion process. The process took only a few minutes to obtain $Ce_{1-x}Sm_xO_{2-1/2x}$ powders. $Ce_{1-x}Sm_xO_{2-1/2x}$ ceramics prepared by microwave-induced process sintered at 1400 °C for 3 h, the bulk density of $Ce_{1-x}Sm_xO_{2-1/2x}$ ceramics were over 95% of the theoretical density. The results revealed that $Ce_{0.84}Sm_{0.16}O_{1.92}$ possessed the maximum electrical conductivity was 0.0287 S cm^{-1} at 850 °C and the minimum activity energy, E_a was 0.9565 eV determined from 500 to 850 °C.

Keywords: Microwave-induced combustion; Solid oxide fuel cell; Nanopowder

1. Introduction

Nanopowders have many excellent properties suited for various applications such as ceramics, gas sensor, rechargeable ceramic batteries, ceramic fuel cells, and so on. In addition, they can significantly enhance sintering rates, decrease sintering temperature, and improve optical, electric, and magnetic properties compared to the micrometer size powders [1,2]. Solid oxide fuel cells are attracting widespread attention due to their high-energy conversion efficiency and low pollution. The high oxide ionic conducting solid electrolyte based on zirconia has been intensively investigated in the pass [3,4]. In order to reduce the operation temperature from 1000 to 800 °C or even lower, doped ceria has been considered as the solid electrolyte for moderate temperature solid oxide fuel cells [5].

In current research, we have attempted a new method, the microwave-induced combustion synthesis process to produce $Ce_{1-x}Sm_xO_{2-1/2x}$ nanopowder. The microwave-induced combustion synthesis process involves the dissolution metal nitrate and urea in water, and then heating of the solution in a microwave oven. After the solution reaches the point of spontaneous combustion, it begins burning and becomes a solid, which burns at high temperature. Combustion is not complete until all the flammable substances are consumed, and the resulting material is a loose, highly friable substance exhibiting voids and pores formed by the escaping gases during the combustion reaction [6]. The whole process takes only a few minutes to yield $Ce_{1-x}Sm_xO_{2-1/2x}$ nanopowders.

2. Experimental procedures

2.1. Sample synthesis

The synthesis process involved the combustion of redox mixtures, in which metal nitrate acted as an oxidizing reactant and urea as a reducing one. This was based on the total oxidizing and reducing valences of the oxidizer and the fuel using the concepts of the propellant chemistry [7].

Stoichiometric amounts of cerium(III) nitrate hexahydrate ($Ce(NO_3)_3{\cdot}6H_2O$), samarium(III) nitrate hexahydrate ($Sm(NO_3)_3{\cdot}6H_2O$), and urea ($CO(NH_2)_2$) dissolved in a minimum quantity of water, were placed in a crucible. The crucible containing the solution was introduced into a microwave oven (CEM, MDS 81D, 650 W). Initially, the solution boils and undergoes dehydration followed by decomposition with the evolution

* Corresponding author. Tel.: +886 3 863 4209; fax: +886 3 863 4200.
E-mail address: d887503@alumni.nthu.edu.tw (Y.-P. Fu).

0378-7753/$ – see front matter © 2006 Elsevier B.V. All rights reserved.
doi:10.1016/j.jpowsour.2006.04.053

of large amount of gases. After the solution reaches the point of spontaneous combustion, it begins burning and releases lots of heat, vaporizes all the solution instantly and becomes a solid burning at high temperature. The powder samples prepared by microwave-induced combustion process were palletized and sintered at 1400 °C for 3 h. The sintered samples were over 95% of the theoretical density in all specimens.

2.2. Characterization measurements

A computer-interface X-ray powder diffractometer (XRD) with Cu Kα radiation was used to identify the crystalline phase. The morphological features of the particle were observed using a scanning electron microscope (SEM). For sintered specimens, the electrical conductivity was measured by two-point dc method on a sintered $Ce_{1-x}Sm_xO_{2-1/2x}$ pellet. The two electrodes were formed by applying platinum paste to the two ends of the pellet and firing at 800 °C for 1 h. The electrical conductivity measurements were made at various temperatures in the range of 500–850 °C in air. Arrhenius plots (plots of $\log\sigma$ versus $10^3/T$) were constructed and activation energies for conduction were computed. The densities of sintered ceramics were measured by the Archimendean method.

3. Results and discussion

The X-ray diffraction patterns of the $Ce_{1-x}Sm_xO_{2-1/2x}$ powders prepared by microwave-induced combustion process were identified by the diffractometer. The particle size, D_{XRD} was calculated according to Scherer equation [8]: $D_{XRD} = 0.9\lambda/B\cos\theta$, where λ is the wavelength of the radiation, θ the diffraction angle, and B is the corrected half-width of the diffraction peak, give by $B^2 = B_m^2 - B_s^2$, where B_m is the measured half-width of the diffraction peak and B_s is the half-width of a standard CeO_2 with a crystal size greater than 100 nm. The particle size determined from the broadening curve is about 14–20 nm in $Ce_{1-x}Sm_xO_{2-1/2x}$ samples. Fig. 1 displays the XRD pattern of $Ce_{1-x}Sm_xO_{2-1/2x}$ ceramics prepared by microwave-induced combustion process in the Sm substitution in range of $x = 0.04$–0.20. The sintered $Ce_{1-x}Sm_xO_{2-1/2x}$ ceramics contain only the cubic fluorite structure for all specimens. Fig. 2 represents scanning electron micrograph of $Ce_{0.84}Sm_{0.16}O_{1.92}$ powders and sintered specimens. As shown in Fig. 2(a), $Ce_{0.84}Sm_{0.16}O_{1.92}$ powders prepared by microwave-induced combustion had a uniform particle sizes distribution and well crystalline shape. Similar images are also found in the other Sm substitution for $Ce_{1-x}Sm_xO_{2-1/2x}$ powders. The particle size obtained by SEM does not depend on the amount of samarium dopant. The van der Waals force can be responsible for the formation of agglomerates of $Ce_{0.84}Sm_{0.16}O_{1.92}$ powders. Fig. 2(b) reveals that sintered $Ce_{0.84}Sm_{0.16}O_{1.92}$ specimen presents uniform grain size ~0.4 μm, high dense microstructure with little closed pores.

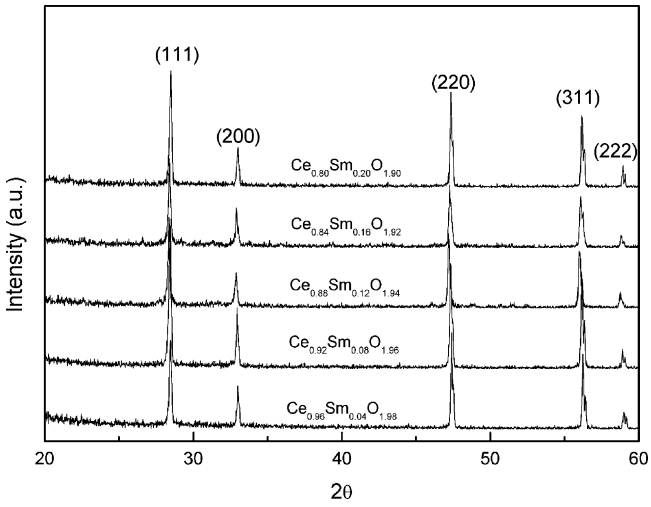

Fig. 1. XRD patterns of $Ce_{1-x}Sm_xO_{2-1/2x}$ ceramics sintered at 1400 °C for 3 h.

The introduction of Sm_2O_3 into CeO_2 can cause a small shift in the ceria peaks. This shift is indicative of change in lattice parameter. Fig. 3 shows the lattice constant of $Ce_{1-x}Sm_xO_{2-1/2x}$ ceramics as a function of dopant concentration, x. Calculation of the cell parameters was carried out using the four main reflections typical of a fluorite structure material with a fcc cell, corresponding to the (1 1 1), (2 0 0), (2 2 0), and (3 1 1) planes. The lattice constant increased with increasing samarium amount. It indicates different radii of Ce^{4+} (0.90 Å) and

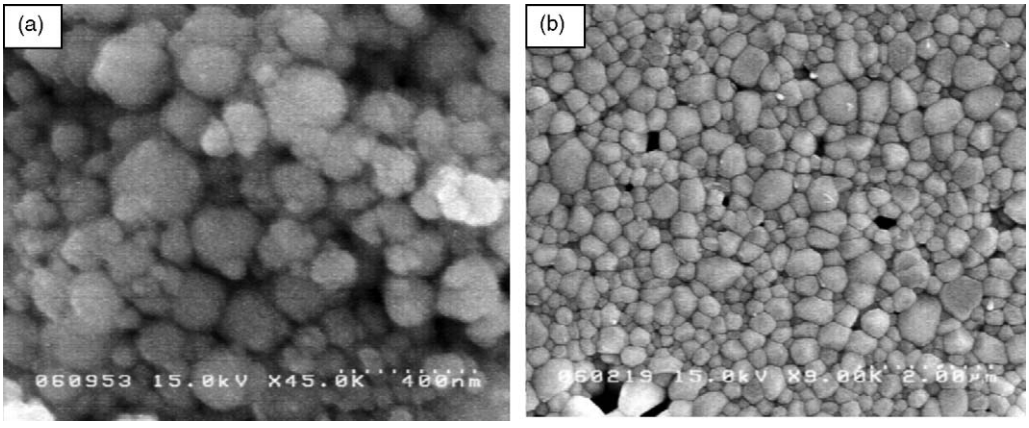

Fig. 2. Scanning electron micrograph of $Ce_{0.84}Sm_{0.16}O_{1.92}$ (a) powder prepared by microwave-induced combustion process and (b) ceramic sintered at 1400 °C for 3 h.

Table 1
Relative density, electrical conductivity, and activation energy of $Ce_{1-x}Sm_xO_{2-1/2x}$ ceramics

Composition	Relativity density (%)	Conductivity (S cm^{-1})			Activation energy (eV)
		650 °C	750 °C	850 °C	
$Ce_{0.96}Sm_{0.04}O_{1.98}$	95.22	6.57×10^{-4}	2.71×10^{-3}	9.72×10^{-3}	1.2212
$Ce_{0.92}Sm_{0.08}O_{1.96}$	96.71	1.83×10^{-3}	8.13×10^{-3}	2.38×10^{-2}	1.1699
$Ce_{0.88}Sm_{0.12}O_{1.94}$	95.58	3.28×10^{-3}	1.06×10^{-3}	2.67×10^{-2}	1.0226
$Ce_{0.84}Sm_{0.16}O_{1.92}$	95.84	2.87×10^{-3}	1.06×10^{-2}	2.87×10^{-2}	0.9565
$Ce_{0.80}Sm_{0.20}O_{1.90}$	96.87	3.42×10^{-3}	1.10×10^{-2}	2.61×10^{-2}	0.9672

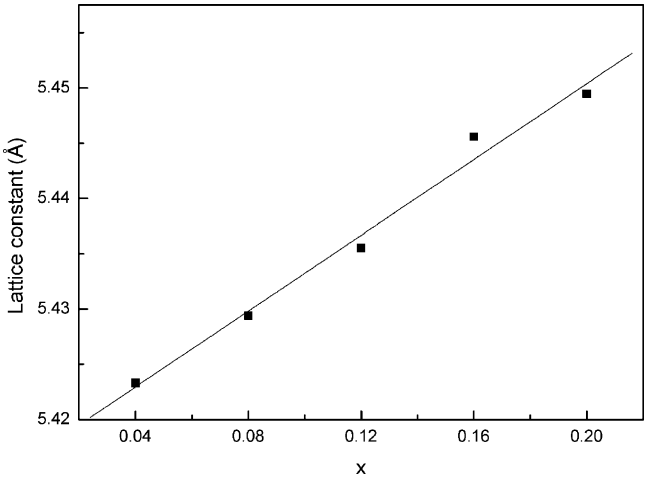

Fig. 3. Lattice constant of $Ce_{1-x}Sm_xO_{2-1/2x}$ ceramics as a function of samarium substitution.

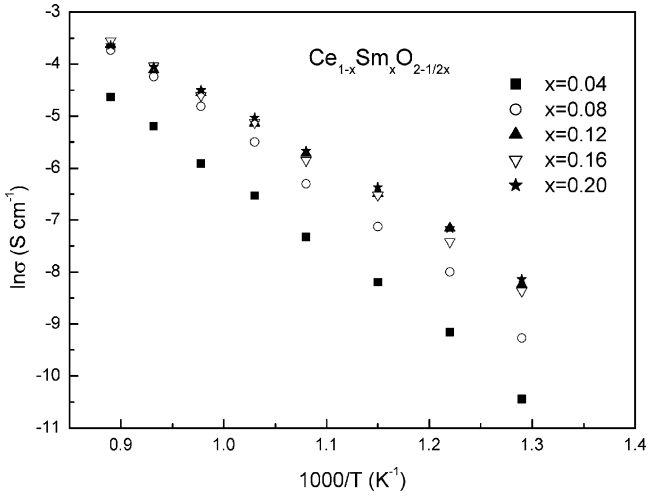

Fig. 4. Arrhenius plots for electrical conductivity of $Ce_{1-x}Sm_xO_{2-1/2x}$ ceramics.

Sm^{3+} (1.11 Å) in an oxide solid solution with a fluorite-type structure. When doped Sm^{3+} ions with larger sized in CeO_2 lattice, cause the fluorite-type structure swell. This effect causes the lattice plane spacing to change and the diffraction peaks to shift to new 2θ position. As the Sm content increases, the lattice constant increases linearly as $a(x) = 5.41608 + 0.1715x$ for $Ce_{1-x}Sm_xO_{2-1/2x}$ ceramics ($x = 0.04$–0.20).

Pure CeO_2 ceramics is a poor oxide ion conductor. However, the ion conductivity can significant improve by increasing the oxygen vacancies by the substitution of samarium, which is lower than 4+ in valence and upon substituting for Ce^{4+} are charge compensated by oxygen vacancies, for example,

$$Sm_2O_3 \xrightarrow{CeO_2} 2Sm'ce + 3O^x o + V\cdots o$$

The electrical conductivity of $Ce_{1-x}Sm_xO_{2-1/2x}$ ceramics as a function of temperature is plotted in Fig. 4. It indicates that the maximum electrical conductivity of the sintered specimens was 0.0287 S cm^{-1} at 850 °C for $Ce_{0.84}Sm_{0.16}O_{1.92}$ specimen. The ionic conductivity of $Ce_{1-x}Sm_xO_{2-1/2x}$ ceramics initially increases with increasing samarium substitution and reaches a minimum at $x = 0.16$. Further increasing the samarium amount for $x > 0.16$ leads to a rise in ionic conductivity.

A summary of relativity density, electrical conductivity, and activation energy of $Ce_{1-x}Sm_xO_{2-1/2x}$ ceramics sintered at 1400 °C for 3 h is listed in Table 1. It depicts that sintered $Ce_{1-x}Sm_xO_{2-1/2x}$ samples were over 95% of the theoretical density in all specimens. The $Ce_{1-x}Sm_xO_{2-1/2x}$ powders synthesized by microwave-induced combustion process can significantly decrease the sintering temperature of $Ce_{1-x}Sm_xO_{2-1/2x}$ ceramics, compared to that above 1550 °C required for ceria solid electrolytes prepared by solid state reaction.

4. Conclusions

Recently, $Ce_{1-x}Sm_xO_{2-1/2x}$ powders have been studied widely due to it is a very important material of solid oxide fuel cells. In this study, using cerium(III) nitrate hexahydrate, samarium(III) nitrate hexahydrate, and urea as the starting materials, nano-size $Ce_{1-x}Sm_xO_{2-1/2x}$ powders have been synthesized successfully by microwave-induced combustion process. The synthesized $Ce_{1-x}Sm_xO_{2-1/2x}$ powders reveal nanodimension and high specific surface. $Ce_{1-x}Sm_xO_{2-1/2x}$ ceramics prepared by microwave-induced combustion process sintering at 1400 °C for 3 h, the highest conductivity was 0.0287 S cm^{-1} at 850 °C and the minimum activation energy, E_a was 0.9565 eV for $Ce_{0.84}Sm_{0.16}O_{1.92}$ specimen. These $Ce_{1-x}Sm_xO_{2-1/2x}$ ceramics with high conductivity are suitable for solid oxide fuel cells applications.

Acknowledgement

The authors would like to thank the National Science Council of the Republic of China for financially supporting this research under Contract No. NSC 93-2212-E-259-001.

References

[1] H. Hahn, J. Mater. Res. 5 (1990) 609.
[2] Y.C. Zhou, M.N. Rahaman, J. Mater. Res. 8 (1993) 1680.
[3] E. Subbarao, H.S. Maiti, Solid State Ionic 11 (1984) 317.
[4] B.C.H. Steele, J. Power Sources 49 (1994) 1.
[5] N.Q. Minh, J. Am. Ceram. Soc. 76 (3) (1993) 563.
[6] O.A. Lopez, J. McKittrick, L.E. Shea, J. Lumin. 71 (1997) 1.
[7] S.R. Jain, K.C. Adiga, V.R.P. Verneker, Comb. Flam. 40 (1981) 71.
[8] H.P. Klug, L.E. Alexander, X-Ray Diffraction Procedures, Wiley, New York, 1974.